

4-2017

Particle Size of Milk Protein Concentrate Powder Affects the Texture of High-Protein Nutrition Bars During Storage.

Justin C. Banach
Iowa State University

Stephanie Clark
Iowa State University FSHN, milkmade@iastate.edu

Buddhi P. Lamsal
Iowa State University, lamsal@iastate.edu

Follow this and additional works at: https://lib.dr.iastate.edu/fshn_ag_pubs

 Part of the [Food Chemistry Commons](#), [Food Microbiology Commons](#), [Food Processing Commons](#), [Human and Clinical Nutrition Commons](#), and the [Molecular, Genetic, and Biochemical Nutrition Commons](#)

The complete bibliographic information for this item can be found at https://lib.dr.iastate.edu/fshn_ag_pubs/206. For information on how to cite this item, please visit <http://lib.dr.iastate.edu/howtocite.html>.

This Article is brought to you for free and open access by the Food Science and Human Nutrition at Iowa State University Digital Repository. It has been accepted for inclusion in Food Science and Human Nutrition Publications by an authorized administrator of Iowa State University Digital Repository. For more information, please contact digirep@iastate.edu.

Particle Size of Milk Protein Concentrate Powder Affects the Texture of High-Protein Nutrition Bars During Storage.

Abstract

Milk protein concentrate powder with 85% protein (MPC85) was jet-milled to give 2 particle size distributions (that is, JM-Coarse and JM-Fine) or freeze-dried (FD), in order to improve the functional properties of MPC85 for use in high-protein nutrition (HPN) bars. Volume-weighted mean diameter decreased from 86 μm to 49, 22, and 8 μm in FD, JM-Coarse, and JM-Fine, respectively ($P < 0.05$). The MPC85 powders modified by jet-milling and freeze-drying were significantly denser than the control MPC85 ($P < 0.05$). Volume of occluded air in the modified powders decreased ($P < 0.05$) by an order of magnitude, yet only FD possessed a lower volume of interstitial air ($P < 0.05$). Particle size reduction and freeze-drying MPC85 decreased its water holding capacity and improved its dispersibility by at least 20%. Contact angle measurements showed that these modifications increased initial hydrophobicity and did not improve wettability. HPN bars made from JM-Fine or FD were firmer by 40 or 17 N, respectively, than the control on day 0 ($P < 0.05$). HPN bar maximum compressive force increased by 38%, 33%, and 242% after 42 d at 32 °C when formulated with JM-Fine, FD, or control MPC85, respectively. HPN bars prepared with JM-Fine were less crumbly than those formulated with control or FD MPC85. Physically altering the particle structure of MPC85 improved its ability to plasticize within HPN bars and this improved their cohesiveness and textural stability.

Keywords

Cohesiveness, freeze-drying, jet-milling, protein bar, texture profile analysis (TPA)

Disciplines

Food Chemistry | Food Microbiology | Food Processing | Food Science | Human and Clinical Nutrition | Molecular, Genetic, and Biochemical Nutrition

Comments

This accepted article is published as Banach, J.C., Clark, S. and Lamsal, B.P.* 2017. Particle Size of Milk Protein Concentrate Powder Affects the Texture of High-Protein Nutrition Bars During Storage. *Journal of Food Science*, 82 (4): 913-921. DOI: [10.1111/1750-3841.13684](https://doi.org/10.1111/1750-3841.13684). Posted with permission.

**Particle Size of Milk Protein Concentrate Powder Affects the Texture of High-protein
Nutrition Bars during Storage**

Banach, J.C., Clark, S., and Lamsal, B.P.*

Iowa State University
Food Science and Human Nutrition
2312 Food Sciences Building
Ames, IA 50011

*Corresponding author: p: 515-294-8681, lamsal@iastate.edu

Desired section: Food Engineering and Materials Science

Title short version: MPC particle size affects bar texture

Word count (title page through references): 6,600

Abstract

Milk protein concentrate powder with 85% protein (MPC85) was jet-milled to give two particle size distributions (i.e., JM-Coarse and JM-Fine) or freeze-dried (FD), in order to improve the functional properties of MPC85 for use in high-protein nutrition (HPN) bars. Volume-weighted mean diameter decreased from 86 micron to 49, 22, and 8 micron in FD, JM-Coarse, and JM-Fine, respectively ($P < 0.05$). The MPC85 powders modified by jet-milling and freeze-drying were significantly denser than the control MPC85 ($P < 0.05$). Volume of occluded air in the modified powders decreased ($P < 0.05$) by an order of magnitude, yet only FD possessed a lower volume of interstitial air ($P < 0.05$). Physical modifications like particle size reduction or freeze-drying of MPC85 decreased water holding capacity and improved dispersibility by at least 20%. Contact angle measurements showed that these modifications increased initial hydrophobicity, yet did not improve wettability. HPN bars made from FD or JM-Fine were firmer by 40 or 17 N, respectively, than the control on day 0 ($P < 0.05$). HPN bar maximum compressive force increased by 38, 33, and 242% after 42 days at 32°C when formulated with FD, JM-Fine, or control MPC85, respectively. HPN bars prepared with JM-Fine were less crumbly than those formulated with control or FD MPC85. Physically altering the particle structure of MPC85 improved its ability to plasticize within HPN bars and this improved their cohesiveness and textural stability.

Keywords: Jet-milling, freeze-drying, protein bar, texture profile analysis (TPA), cohesiveness

Practical Application

Milk protein concentrate (MPC) powder particle size significantly influences the texture of high-protein nutrition (HPN) bars. Use of finely jet-milled MPC85 powder produced HPN bars with increased firmness and cohesiveness. Particle size reduction improved the textural stability of MPC-formulated HPN bars and this physical modification has the potential to extend sensory shelf life of such products.

Introduction

The main function of protein in nutritional bars, specifically high-protein nutrition (HPN) bars, is to nurture the consumer. Formulating HPN bars with 20-50% protein (w/w) is a challenge as inclusion at these levels adversely affects texture and shortens sensory shelf life. High-protein (i.e., $\geq 80\%$ protein w/w) milk protein concentrate (MPC) powders produce HPN bars that quickly harden during storage and lack cohesion (Loveday and others 2009; Imtiaz and others 2012; Banach and others 2016a). Whey protein concentrate (WPC) or isolate (WPI), specifically their hydrolysates, produce texturally stable HPN bars (McMahon and others 2009). Food protein hydrolysates advantageously possess lower glass transition temperature (T_g) compared to their intact counterparts, which allows for better protein powder plasticization during HPN bar production and enables the resultant soft, rubbery state to be maintained throughout storage (Rao and others 2016b). On a protein basis, MPCs concentrated from bovine skim milk contain $\sim 80\%$ casein and $\sim 20\%$ whey. Since the caseins have higher molecular weight than the dominant whey proteins (i.e., β -lactoglobulin, α -lactalbumin) (O'Mahony and Fox 2013), MPCs have higher T_g than whey based ingredients with similar protein concentration. The glass-rubber transition temperature (T_{gr}), a thermo-mechanically determined T_g analogue, of MPC increased with its protein concentration (Kelly and others 2015). From a functionality

standpoint, this means that high-protein MPC powder particles resist collapse and maintain their structure when used in HPN bars (Hogan and others 2016). The structural properties of whey protein based powders have not been studied in terms of their effect on HPN bar texture since particles are more likely to become fully plasticized within such products. However, these properties require consideration when formulating HPN bars with high-protein MPC.

Particle size and distribution, shape, and surface composition are some of the properties that influence protein powder functionality in semi-solid intermediate moisture foods (IMF) (Huppertz and Hogan 2015; Li and others 2016). The effects of these properties on MPC functionality, especially its performance in HPN bars, have not been considered by most preceding studies. High-fructose corn syrup (HFCS) and other polyols (e.g., glycerol) are used in HPN bars to bind the system together and impart textural stability while maintaining microbe-inhibiting water activity ($a_w \leq 0.65$) (Liu and others 2009). Small polydisperse particles required a larger volume fraction than large uniformly sized particles of the same WPI powder to solidify an experimental HFCS-WPI system (Hogan and others 2016). Agglomerated micellar casein concentrate (MCC) particles produced HPN bars that were powdery and texturally more stable than the dough-like control formulated with non-agglomerated MCC (Hogan and others 2012). Fat and protein preferentially exist on the exterior of spray dried MPC powder particles whereas more hydrophilic components, namely lactose and minerals, are interiorly located (Kelly and others 2015). Modifications that affect the particle size distribution or expose components that assist with hydration of MPC will have an effect on the textural properties of HPN bars that it is used to make.

Size reduction of powder particles alters structure, functionality, and performance in food applications. Jet-milling of wheat flour increased its water holding capacity (WHC) and

lightened its color (Protonotariou and others 2014). Jet-milled flour produced texturally harder bread with lower volume, luminosity, moisture, and glycemic index compared to the un-milled control (Protonotariou and others 2015). Superfine soy flour had higher WHC, solubility, swelling, fat binding, and sensory scores compared with the control (Muttakin and others 2015). Milling WPC increased its solubility, hydrophobicity, oil binding capacity, and foaming properties, but decreased its WHC (Sun and others 2015a, 2015b). Surface hydrophobicity of acid casein and egg white powder increased as particle size decreased (Hayakawa and others 1993). Ball-milling can produce superfine protein powders on a laboratory-scale (Sun and others 2015b), but batch operation and longer processing times make it an impractical unit operation for industrial scale-up. Alternatively, jet-mills offer continuous throughput and media-less attrition by particle-particle and particle-wall collisions induced by high velocity airflow (Saleem and Smyth 2010). Jet-milling can also alter particle structure, and hence functionality, through application of compressive and shear forces (Hayakawa and others 1993). It is currently unknown how particle size reduction via jet-milling will affect the functional properties of high-protein MPC or its performance in HPN bars.

Literature discussions of protein functionality focus on protein solubility and solubility-dependent properties (e.g., emulsification, foaming). Such properties are directly relevant in liquid (e.g., beverages) and semi-liquid (e.g., soft gels, yogurt) food applications. Poorly soluble protein powders are problematic for beverages. However, HPN bars made from soy protein powder with intermediate solubility (i.e., $30\% < \text{soluble solids index} < 50\%$) were softer than those made from a more soluble source (i.e., $\text{soluble solids index} > 50\%$) (Cho 2010). Properties other than solubility, such as WHC and surface hydrophobicity, need consideration in low moisture (e.g., protein powders) and IMFs (e.g., HPN bars). Proteins with high WHC are

thought to pull water from other components during HPN bar storage. This redistribution of water is a commonly proposed mechanism for time-dependent texture change (Cho 2010; Hazen 2010). Protein powder WHC and surface hydrophobicity are influenced by particle size reduction (Hayakawa and others 1993; Sun and others 2015a, 2015b). Hydrophobic protein powder particles may slow hydration during HPN bar manufacture, but may also help inhibit moisture migration during storage. Particle size and structure of MPC with 85% protein (MPC85) was modified by jet-milling or freeze-drying in the present study. Then HPN bar relevant functionalities were measured to explain textural and stability differences between model HPN bars formulated with each powder.

Materials and Methods

Study Design

The study consisted of three parts: 1) MPC85 modification, 2) functional property evaluation, and 3) textural evaluation of a model HPN bar system. Jet-milling or freeze-drying were used to physically modify MPC85. Two levels of jet-milling, based on the resultant particle size of MPC85, were evaluated: i.e. fine milled (JM-Fine) and coarse milled (JM-Coarse). Only one level for the freeze-drying (FD) modification was evaluated. These MPC85 modifications were conducted once. Dependent variables measured pre- and post-modification include: particle size distribution D-values (i.e., D_{10} , D_{50} , D_{90} , $D_{4,3}$) and span, loose (ρ_{loose}), tapped (ρ_{100X}), extremely tapped (ρ_{1250X}), and particle ($\rho_{particle}$) densities, occluded (V_{oa}) and interstitial (V_{ia}) air volumes, WHC, dispersibility index (DI), initial (θ_{0s}) and final (θ_{420s}) water droplet contact angle, initial (V_{0s}) and final (V_{420s}) water droplet volume, and the rate of change for contact angle ($d\theta/dt$) and water droplet volume (dV/dt). These properties and functionalities were used to explain textural and stability differences between HPN bars formulated with

control, JM-Fine, or FD MPC85. The HPN bars were stored at 2 temperatures (i.e., 22°C or 32°C) and were evaluated at 6 time points (i.e., days 0, 6, 13, 20, 29, and 42). Dependent variables for the HPN bars include hardness, fracturability, maximum compressive force, adhesiveness, crumbliness, water activity (a_w), moisture content, and density. The HPN bars were prepared, stored, and evaluated three separate times.

Materials

MPC85 (NutraPro®85 containing 85.2% protein, 4.3% moisture, 1.9% fat, 7.0% ash, and 1.6% lactose) was obtained from Grassland Dairy Products, Inc. (Greenwood, WI). Corn maltodextrin (Maltrin®180 containing 16.5-19.9 dextrose equivalents and 6% moisture) came from Grain Processing Corporation (Muscatine, IA). HFCS (CornSweet®55 containing 55% fructose, 41% dextrose, 4% higher saccharides, and 23% water) and low-viscosity liquid lecithin (Beakin®LV1 with 0.8% moisture) were provided by Archer Daniels Midland (Decatur, IL). Maltitol syrup (Lycasin®80/55 containing 51.7% D-maltitol, 3.0% D-sorbitol, and 24.5% water) was from Roquette America (Keokuk, IA). Non-hydrogenated trans-free palm oil (SansTrans®39) was from IOI Loders Croklaan (Channahon, IL). Glycerol (99.8% pure with 0.1% water) was purchased from Fisher Scientific (Waltham, MA). Millipore water had resistivity of 18.2 M Ω ·cm at 25°C.

Jet-milling and Freeze-drying MPC85

MPC85 was jet-milled by Aveka CCE Technologies (Cottage Grove, MN) with an Aveka 100/20 jet-mill/air classifier system. JM-Coarse and JM-Fine were obtained at classifier rotor speeds of 1,000 and 2,500 rpm, respectively. Separately, MPC85 was rehydrated at 5% protein (w/w) in room temperature Millipore water with continual overhead mixing for 2 h. After holding the solution for 5 h at 4°C, it was frozen (-20°C) and freeze-dried (VirTis Genesis 25 LE,

SP Scientific, Warminster, PA). Freeze-dried material was mechanically milled into the FD sample using a L'Equip NutriMill (St. George, UT).

Protein Powder Characterization and Functional Property Evaluation

Protein content was measured ($n = 2$) by Dumas nitrogen combustion (AOAC 1998). Moisture content was determined ($n = 3$) by mass difference after drying for 16 h at 102°C. Particle size D-values and distribution span were measured ($n = 2$) by laser diffraction (Mastersizer 2000, Malvern Inc., Worcestershire, United Kingdom) (Banach and others 2016a). Loose (ρ_{loose}), tapped (ρ_{100x}), and extremely tapped (ρ_{1250x}) densities were calculated ($n = 3$) after mechanically tapping (Autotap™, Quantachrome Instruments, Boynton Beach, FL) 30 g powder in a 100-mL graduated glass cylinder 0, 100, and 1,250 times, respectively. Particle density (ρ_{particle}) was measured ($n = 2$) with a helium pycnometer (G-DenPyc 2900, Gold APP Instruments Corporation, Beijing, China). Interstitial ($V_{\text{ia}} = 100/\rho_{100x} - 100/\rho_{\text{particle}}$) and occluded ($V_{\text{oa}} = 100/\rho_{\text{particle}} - 100/\rho_{\text{solids}}$) air volumes (mL/100 g) were calculated. MPC85 solids density (ρ_{solids}) was 1.39 g/cm³ (Crowley and others 2014; Walstra and others 2005). WHC was evaluated ($n = 3$) by the water saturation technique following Quinn and Paton (1979). Ten g of protein powder was added to 100 mL Millipore water and was stirred with a spatula for 25 s. Protein-water dispersions were poured through a 212-micron mesh and dispersion index (DI) was the percent solids in the filtrate ($n = 3$) (Schuck and others 2012; Bouvier and others 2013).

Surface hydrophobicity and wettability were probed ($n = 4$) by measuring the dynamic contact angle and volumetric absorption of water on pressed surfaces made from each powder. Powder (0.10 g) was loaded into a 13-mm pellet die (model 3619, Carver, Inc., Wabash, IN) and was pressed (model 4350, Carver, Inc., Wabash, IN) at 8,000 kg_f for 2 min. A 4 μL droplet of Millipore water was placed on the pressed surface using a micrometer syringe (Gilmont GS-

1200, Cole-Parmer, Vernon Hills, IL) and images were captured every 0.1, 1, and 10 s between 0-1, 1-10, and 10-420 s, respectively, using a goniometer (model 250, Ramé-hart Instrument Co., Succasunna, NJ). Images were reprocessed in DROPimage® software (version 2.8.02, University of Oslo, Norway) and mean contact angle (°), surface droplet volume (μL), and volume percent remaining were reported.

Model High-protein Nutrition Bar Preparation

HPN bars (700 g) were prepared at 30% protein (w/w) using either control, JM-Fine, or FD MPC85. HFCS (39.6 g), glycerol (146.1 g), maltitol syrup (72.5 g), and distilled water (50.2 g) were heated to 60°C and were then combined with melted palm oil (105.1 g) and lecithin (3.5 g) (Banach and others 2016a). Protein powder (248 g) blended with maltodextrin (35.1 g) was intermittently added to the lipid/polyol blend over 4.5 min of low-speed mixing with the paddle attachment using a stand mixer (K5SS, Kitchen Aid, St. Joseph, MI). HPN bar dough was pressed to fixed height (15.5 mm ± 0.5 mm) and cylindrical (dia. = 19.1 mm) samples were cut. Separately HPN bar dough was hand-pressed into water activity sample cups. All samples were sealed in metallized bags (S-16891, Uline, Pleasant Prairie, WI).

High-protein Nutrition Bar Testing

HPN bar samples (n = 6) from each powder, temperature, time, and preparation combination were twice compressed to 60% strain at 2 mm/s using the TA-XT2 Texture Analyzer (Texture Technologies, Scarsdale, NY) (Banach and others 2016a). Hardness (N) was the force at maximum strain. Fracturability (N) was the force required for the sample to yield or crack. Maximum compressive force (N) was the larger value for each measurement. Adhesiveness (J) was the absolute area under the curve generated during the first crosshead withdrawal. Following compression, the samples were sieved three at a time by mechanical

shaking for 30 s on speed 3 (Shaker #18480, CSC Scientific Sieve, Fairfax, VA). Crumbliness was the mass percent passing the top mesh with 5.6 mm aperture (Banach and others 2016a). Water activity (a_w) was measured ($n = 3$) using the Aqua Lab 4TE Duo (Decagon Devices Inc., Pullman, WA). Moisture content was calculated after oven drying 1 g samples ($n = 3$) at 102°C for 26 h. On day 42, HPN bar density was calculated ($n = 6$). Least squares means for texture, water activity, and moisture content were reported. Means for the texture profile analysis (TPA) generated attributes were used to calculate percent change from day 0.

Statistical Analyses

The generalized linear mixed model (GLMM) (SAS® software, version 9.4, SAS Institute Inc., Cary, NC) was used to determine the significance of difference between least squares means for the protein powder properties. Measurement replicate was set as the random error term. Protein powder, time, and their interaction were independent variables and sample replicate was the random error term in models comparing contact angle and water droplet volume. These latter two response variables were also modeled with time as a continuous variable to compare each average rate of change (i.e., $d\theta/dt$ and dV/dt) with simulate correcting for multiplicity. Least squares means for HPN bar properties were calculated and compared using the GLMM. HPN bar preparation was set as the random error term. Slicing factors were applied to make statistical comparisons at fixed temperature and time (i.e., columns in Tables 4-7) and across the entire storage period (i.e., rows in Tables 4-7). The latter comparison assumes 6 d storage at 32°C approximates 7.4 weeks at 22°C (Li and others 2008; McMahon and others 2009) and that each subsequent evaluation at the elevated temperature simulates more lengthy storage. All contrasts were evaluated at $\alpha = 0.05$ using Tukey's adjusted P -value unless another adjustment was specified.

Results and Discussion

Powder Protein and Moisture Content

Jet-milling or freeze-drying MPC85 did not change its average as-is protein content (84.5%). Moisture content of FD (1.6%) was lower ($P < 0.05$) than the control (2.6%), JM-Coarse (3.5%), and JM-Fine (3.1%). Moisture contents of the latter three powders did not differ significantly ($P > 0.05$). Freeze-drying allowed for more thorough dehydration. High airflow and exposure to elevated temperature during jet-milling did not change the moisture content of MPC85.

Powder Particle Sizes, Densities, and Air Volumes

Jet-milling or freeze-drying MPC85 reduced its particle size. All particle size D-values decreased ($P < 0.05$) in the order of control, FD, JM-Coarse, and JM-Fine (Table 1). Volume-weighted mean diameter ($D_{4,3}$) of control MPC85 was 25 μm larger than previously analyzed MPC80 ($D_{4,3} = 61 \mu\text{m}$) (Banach and others 2016a) and 55 μm larger than previously analyzed MPC85 ($D_{4,3} = 31 \mu\text{m}$) (Kelly and others 2015). Particle size differences between spray dried powders are attributed to inlet stream properties (e.g., percent solids, viscosity) and drying conditions (e.g., inlet and outlet temperature, atomization) (Chew and others 2014). Increasing classifier speed from 1,000 (i.e., JM-Coarse) to 2,500 (i.e., JM-Fine) rpm decreased $D_{4,3}$ by 14 μm . MPC85s with the same proximate composition, but different size distributions will likely have altered functionalities. For example, casein-based powder (e.g., MPC, MCC) solubility is limited by dissolution rather than wetting and hence smaller sized particles are recommended to improve this property (Schuck and others 2007).

Particle size reduction or freeze-drying increased the ρ_{loose} of JM-Fine and FD ($P < 0.05$) compared to the statistically equivalent JM-Coarse and control (Table 1). Control, JM-Fine, and

JM-Coarse ρ_{100X} values were statistically equivalent ($P > 0.05$). The ρ_{1250X} values for the jet-milled MPC85s were about 0.07 g/cm^3 greater than the control ($P < 0.05$). FD particles had similar size as the control, but ρ_{loose} , ρ_{100X} , and ρ_{1250X} were each significantly greater ($P < 0.05$). In most instances, these densities of FD were also greater than the values obtained for the jet-milled MPC85s. Jet-milling or freeze-drying MPC85 increased its $\rho_{particle}$ and decreased its V_{oa} ($P < 0.05$) (Table 1). Altered particle structure by freeze-drying reduced V_{ia} ($P < 0.05$) and allowed for less entrained air between powder particles.

Powder Water Holding Capacity and Dispersibility Index

Jet-milling or freeze-drying MPC85 decreased its WHC even though surface area available for water absorption increased (Table 2). Centrifugal force applied during the assay compacted the modified powders more than the control and this decreased space between adjacent particles for water to be held. Modified powder ρ_{1250X} supported this notion of increased compactability since values were significantly greater than the control. Lower V_{oa} in the modified MPC85s provided less inner-particle space for water to be entrapped in sponge-like fashion. Control MPC85 had WHC that was 0.1 g/g higher than unmodified MPC80 since it was comprised of larger particles (unpublished data). The physical characteristics of protein powders, namely size distribution, extremely tapped density, and volume of occluded air, are factors that affect WHC and require consideration when comparing and selecting MPCs.

Jet-milling or freeze-drying MPC85 improved its dispersibility in water ($P < 0.05$), but no significant difference ($P > 0.05$) in DI was found between modifications (Table 2). Protein powder particle size reduction may have increased particle passage through the mesh used for DI determination. Extrusion-porosification of MPC85 reportedly improved its DI from 38% to 96% (Bouvier and others 2013). Pores that formed in FD while freeze-drying rehydrated MPC85 may

have similarly increased its DI. Increasing the DI of these poorly dispersible powders should improve their solubility (Schuck and others 2012; Bouvier and others 2013). In fact, another study found that freeze-dried MPC80 was more soluble between pH 5.5 and 7.0 than the spray-dried control (Banach and others 2013). This was likely due to increased dispersibility. Higher DI may translate into improved dispersibility and rehydration of the modified MPC85s in the lipid/polyol blend during HPN bar production.

Powder Dynamic Contact Angle: Surface Hydrophobicity and Wettability

A water droplet forms a larger contact angle on hydrophobic surfaces than on hydrophilic ones. Based on θ_{0s} values (Table 3), JM-Fine was more hydrophobic than JM-Coarse and FD ($P < 0.05$), but its hydrophobicity did not differ significantly ($P > 0.05$) from the control. Jet-milling increased the surface hydrophobicity of MPC85 through exposure of buried hydrophobic residues as was also reported for acid casein (Hayakawa and others 1993). Water droplet profile change by spread over and absorption into pressed surfaces has been used to describe powder wettability (Alghunaim and others 2016). Contact angle on the control decreased rapidly within the first few seconds, but then it decreased at a rate similar to the droplets on the modified MPC85s (Figure 1A). Contact angle changed faster, based on $d\theta/dt$ values, on JM-fine and the control compared to JM-Coarse and FD, but pairwise differences were insignificant (Table 3). Each powder significantly absorbed, with respect to initial volume, the water droplet after 420 s ($P < 0.05$). Droplet volume rate of change (dV/dt) on JM-Fine was faster compared to FD ($P < 0.05$), but it did not differ significantly with the rates for control or JM-Coarse (Table 3). Droplet volume-percent remaining (Figure 1B) on the control decreased at the beginning of analysis and indicated that water was quickly absorbed. FD did not appear to absorb as much water as the other protein powders (Figure 1B) even though contact angle of the water droplet on

its surface quickly changed during the first second of analysis. At 420 s, the pressed surface and water approached a wetted equilibrium where droplet profile changed at a much slower rate (Figure 1C). At this time, contact angle of the water droplet on the control was smaller than on the modified powders and indicated lower hydrophobicity. Since water droplets remained on all surfaces after 420 s (Figure 1C), it is safe to suffice that jet-milling or freeze-drying MPC85 did little to improve its wettability.

High-protein Nutrition Bar Production

The small MPC85 particles of FD and JM-Fine easily suspended in the lipid/polyol blend. During HPN bar production, dough made from either of these two powders was more fluid than the dough made with the larger particle containing control. However, when sheeted, the JM-Fine dough quickly transitioned from a pourable batter into a solid HPN bar. Solidity was so high that JM-fine HPN bar samples were difficult to punch from the sheet and when expelled from the cutter. Samples cut easily from control and FD HPN bar sheets and maintained their shaped when pushed from cutter (Figure 2).

MPC85 particle size reduction and morphological changes increased HPN bar density. HPN bar mean (\pm SD) density was 0.81 ± 0.01 , 0.96 ± 0.02 , or 0.96 ± 0.01 g/cm³ when formulated with control, FD, or JM-Fine, respectively. Density difference suggests that some particle structure was retained during HPN bar production. When used in a different protein bar formulations, MPC80 also partially maintained its particle structure (Loveday and others 2009). Without structural collapse, the larger particles in the control HPN bar were not able to pack as tightly as the smaller particles did in the HPN bars formulated with JM-Fine or FD. The smaller particles, specifically the fraction with diameter less than or equal to 1 μ m (i.e., D₁₀), in the latter two powders positioned themselves in closer vicinity to each other. Both powders also had

narrower distribution and smaller span (Table 1) than the control ($P < 0.05$), which allowed them to fill void volume better within their respective HPN bars. Additionally, JM-Fine and FD had lower V_{oa} than the control and their use introduced less air into the HPN bar. It was not possible to increase the density of the control HPN bar by pressing more mass into the fixed volume pan.

High-protein Nutrition Bar Water Activity and Moisture Content

Average HPN bar a_w on the day of manufacture was 0.60, and after 42 d at 22°C or 32°C, it marginally increased to 0.61. Storage time had an effect on a_w ($P < 0.05$), but powder, temperature, and all interactions were insignificant ($P > 0.05$). Previously, small yet significant increases in HPN bar a_w during storage suggested that texture changes occur because of water migration from the protein component to the bulk phase (McMahon and others 2009; Banach and others 2014, 2016a). Moisture content of the control HPN bar (26%) was greater than JM-Fine (24%) and FD (24%) on day 0 ($P < 0.05$). There were no significant ($P > 0.05$) changes in HPN bar moisture content during storage and the texture changes reported in the following section are not due to moisture loss. Higher moisture and a_w in the present system, compared with HPN bars formulated with MPC80 (Banach and others 2014, 2016a), might have slowed movement of water molecules between constituents because of smaller internal gradients. Dew point based a_w measurement lacks sensitivity and no detectable change does not fully rule out the occurrence of internal moisture migration.

High-protein Nutrition Bar Texture Change during Storage

Hardness (Table 4), fracturability (Table 5), and maximum compressive force (Table 6) are reported separately because each HPN bar behaved differently during compression. On and after day 29, including all time points at 32°C, every control HPN bar sample fractured and crumbled prior to 60% strain. JM-Fine HPN bars yielded during the first compression and

always obtained maximum compressive force at maximum deformation. FD produced a HPN bar with intermediate fracture behavior. On day 0, all FD samples fractured during the first compression yet maintained maximum compressive force at 60% strain. After 42 d at 22°C or 32°C, 4 of 18 samples or 13 of 18 samples, respectively, required more force to initiate fracture than compress at 60% strain. Interestingly, the force required for fracture was not significantly ($P > 0.05$) affected by the protein powder used and after equivalent storage the HPN bars fractured or yielded under similar load. Hardness and maximum compressive force were influenced by the protein powder ($P < 0.05$), but only the latter texture attribute was significantly affected by time ($P < 0.05$). The only HPN bar for which true hardness significantly increased ($P < 0.05$) during storage was formulated with JM-Fine. HPN bar hardness always increased ($P < 0.05$) in the order of control, FD, and JM-Fine. Maximum compressive force of the control and FD formulated HPN bars were statistically similar throughout storage whereas the one formulated with JM-Fine was always greater than these other two ($P < 0.05$). These differences would have been missed if only one hardening attribute (i.e., hardness, fracturability, or maximum compressive force) were used to describe texture change.

HPN bar adhesiveness (Table 7) decreased and crumbliness (Figure 3) increased during storage ($P < 0.05$). Adhesiveness, the work required to overcome attractive forces between surfaces, was positively and inversely correlated with panelist-perceived cohesiveness and crumbliness, respectively (Banach and others 2016a). However, instrumentally measured crumbliness better represented HPN bar crumbliness/cohesiveness than adhesiveness (Banach and others 2016a). Both adhesiveness and crumbliness were significantly influenced by the formulating powder, storage temperature, and storage time ($P < 0.05$). The control lacked adhesiveness and remained crumbly throughout storage, which aligned with a previously

evaluated HPN bar formulated with MPC80 (Banach and others 2016a). The latter had lower moisture and a_w than the current model HPN bar and yet was less crumbly since prepared with smaller sized powder particles. FD remained more adhesive than the control through 13 d at 32°C ($P < 0.05$) and had slightly lower crumbliness. The JM-Fine HPN bar was more adhesive ($P < 0.05$) and less crumbly than the control and FD throughout storage. Its crumbliness increased from 6% to 17% ($P < 0.05$) after 1 week at 22°C. No significant change in crumbliness for this HPN bar was noted again until day 13 at 32°C, or approximately 16 weeks at 22°C, when it increased to and plateaued at 32%. Smaller particles are by nature more adhesive (Schwarzwälder and others 2014) and this contributed to improved cohesiveness. HPN bars made with smaller and morphologically altered powders, especially JM-Fine, were more adhesive and cohesive than the control formulated with native MPC85.

Particle size reduction by jet-milling and morphological change by freeze-drying influenced initial HPN bar texture and its change during storage. In terms of the hardness attributes, JM-Fine produced the most firm HPN bar. This result aligned with the work of Cho (2010), which found that smaller soy protein powder particles produced firmer HPN bars than powders with larger size. If softer HPN bar texture is desirable, then MPC85 particle size reduction would not be a viable modification to improve its performance. However, based on percent change from initial texture, the TPA attributes of the HPN bars were less prone to change when formulated with JM-Fine or FD compared to the control (Figure 4). This was not apparent for hardness (Figure 4A) itself due to changes in overall texture and behavior under compression after day 0. Fracturability (Figure 4B) and maximum compressive force (Figure 4C) of the control HPN bar increased by 266% and 242%, respectively, when kept at 32°C for 42 d. The respective increases for the JM-Fine HPN bar were 115% and 38%, and for the FD HPN bar

were 128% and 33%. Changes in HPN bar adhesiveness (Figure 4D) were not as large overall, but a greater decrease occurred for the control. Jet-milled or freeze-dried MPC85 produced HPN bars with enhanced textural stability. Jet-milled MPC85 also improved HPN bar cohesion and might be preferred for this reason.

Explanation for Texture Changes in High-protein Nutrition Bars Formulated with High-protein MPCs

Based on present findings and literature, we surmise that high-protein MPC particle structure is partially maintained within the HPN bars (Loveday and others 2009; Banach and others 2014). Particle collapse and fusion into a plasticized mass via particle-particle bridge formation occurs when system temperature exceeds protein powder T_{gr} (Zhou and others 2014; Hogan and others 2016). Compared with lower-protein MPCs, MPC85 had higher T_{gr} , which decreased from $\sim 76^{\circ}\text{C}$ to $\sim 53^{\circ}\text{C}$ as powder a_w increased from 0.11 to 0.44 (Kelly and others 2015). During model HPN bar production, MPC85 powder particles underwent exposure to elevated temperature when mixed into the preheated ($\sim 60^{\circ}\text{C}$) lipid/polyol blend. This allowed for surface rehydration and partial particle collapse. Exposure to elevated temperature was short-lived and with limited free moisture, it was impossible for all particles to proceed through their glass-rubber transition. As a result, MPC85 particles were both structurally intact and partially plasticized within the HPN bars under current study.

The fraction of plasticized versus un-plasticized MPC85 particles influences HPN bar texture. While the control powder had the highest WHC (Table 2) and absorbed water better than powders modified by jet-milling or freeze-drying (Figure 1B), these functionalities did not help produce a cohesive HPN bar. Control MPC85 likely had higher T_{gr} than these modified powders. Particle size reduction by jet-milling or morphological modification by freeze-drying

increased specific surface area for water sorption. This decreased particle T_{gr} , increased the likelihood of their collapse, and improved plasticization when made into HPN bars. Containing a larger fraction of un-plasticized MPC85, the control HPN bar was always the most crumbly (Figure 3). Another HPN bar, in this case formulated with MPC80, possessed lower moisture and water activity than the MPC85-formulated control and yet its crumbliness was lower since the formulating powder had smaller size distribution, and particles were more easily plasticized within the HPN bar (Banach and others 2016a). Un-plasticized MPC particles retain their structure within HPN bars and increase crumbliness.

HPN bar texture changes as the partially plasticized, rubber-like, and chemically reactive proteins return to the glassy state when stored at lower temperature than the T_{gr} . Systems with higher T_{gr} undergo more rapid return to the glassy state and as was the case with the control HPN bar, more pronounced texture change. As protein plasticization was lost during storage, the HPN bars hardened (Figure 4A-C), lost adhesion (Figure 4D), and became more crumbly (Figure 3). Conversely, protein hydrolysates, which have suppressed T_{gr} , produce texturally stable HPN bars that maintain the rubbery state while stored at a temperature greater than their T_{gr} (Rao and others 2016a, 2016b). Protein T_{gr} increases during HPN bar storage as water migrates to other components and as high molecular weight protein aggregates form (Zhou and others 2008a, b; Loveday and others 2010). Increasing T_{gr} accelerates the return of the partially plasticized proteins back to the glassy state and further contributes to HPN bar texture change. Protein powder particles have limited reactivity in this glassy state and consequently chemical change contributes little to the hardening of MPC-formulated protein bars (Loveday and others 2009; Banach and others 2016b). Some chemical changes occur due to the presence of low molecular mobility in this state (Roudaut and others 2004) and since a fraction of the MPC proteins were

plasticized during HPN bar production. It is possible that increases in specific surface area by powder modifications may accelerate chemical reactions, but those analyses are beyond the scope of the current work. Jet-milled or freeze-dried MPC85 produced texturally stable HPN bars by increasing the fraction of plasticized powder, lowering T_{gr} , and slowing the system's return to the glassy state.

Conclusions

MPC powder particle size and shape affect the functional properties and textural performance within HPN bars. Finely jet-milled MPC85 produced HPN bars that were firmer and more cohesive than the control with unmodified MPC85. More importantly, HPN bars formulated with finely jet-milled MPC85 or freeze-dried MPC85 were less prone to texture change during storage. Particle size reduction removed occluded air from the spray dried MPC85 and allowed for denser particle packing in the HPN bars. Reducing the particle size of MPC85 improved its ability to rehydrate during HPN bar production, which translated to improved plasticization and HPN bar cohesion. Particle size, shape, and physical properties should be considered when evaluating the functional properties of protein powder concentrates and their effect on HPN bar texture and its change during storage. A texturally stable, less-crumby HPN bar can be produced with MPC85 if particle size is reduced.

Acknowledgement

Special thanks to Lucas Santos de Jesus for assisting with protein bar production and texture analysis. Dairy Research Institute award #H003889501 through the University of Minnesota and funds provided by the Iowa State University Agricultural Experiment Station supported this work. Thanks are also due to Dr. Hulya Dogan for her help with tapped density measurements for powder samples.

References

- Alghunaim A, Kirdponpattara S, Newby B-mZ. 2016. Techniques for determining contact angle and wettability of powders. *Powder Technol* 287:201-15.
- [AOAC] Assn. of Official Analytical Chemists. 1998. Method 992.23. In: *Official methods of analysis of Assn. of Analytical Chemists*. 16th ed. Arlington, Va.: AOAC.
- Banach JC, Clark S, Lamsal BP. 2016a. Instrumental and sensory attributes of high-protein nutrition bars formulated with extruded milk protein concentrate. *J Food Sci* 81(5):S1254-62.
- Banach JC, Clark S, Lamsal BP. 2016b. Microstructural changes in high-protein nutrition bars formulated with extruded or toasted milk protein concentrate. *J Food Sci* 81(2):C332-40.
- Banach JC, Clark S, Lamsal BP. 2014. Texture and other changes during storage in model high-protein nutrition bars formulated with modified milk protein concentrates. *LWT - Food Sci Tech* 56(1):77-86.
- Banach JC, Lin Z, Lamsal BP. 2013. Enzymatic modification of milk protein concentrate and characterization of resulting functional properties. *LWT - Food Sci Tech* 54(2):397-403.
- Bouvier J-M, Collado M, Gardiner D, Scott M, Schuck P. 2013. Physical and rehydration properties of milk protein concentrates: comparison of spray-dried and extrusion-porosified powders. *Dairy Sci Technol* 93(4):387-99.
- Chew JH, Liu W, Fu N, Gengenbach T, Chen XD, Selomulya C. 2014. Exploring the drying behaviour and particle formation of high solids milk protein concentrate. *J Food Eng* 143:186-94.

- Cho MJ. 2010. Soy protein functionality and food bar texture. In: Cadwallader KR, Chang SKC, editors. *Chemistry, Texture, and Flavor of Soy*. Washington, DC: American Chemical Society. p 293-319.
- Crowley SV, Gazi I, Kelly AL, Huppertz T, O'Mahony JA. 2014. Influence of protein concentration on the physical characteristics and flow properties of milk protein concentrate powders. *J Food Eng* 135:31-8.
- Hayakawa I, Yamada Y, Fujio Y. 1993. Microparticulation by jet mill grinding of protein powders and effects on hydrophobicity. *J Food Sci* 58(5):1026-9.
- Hazen, C. 2010. Texture solutions for snack bars. *Food Product Design*. 6:40-58.
- Hogan SA, O'Loughlin IB, Kelly PM. 2016. Soft matter characterisation of whey protein powder systems. *Int Dairy J* 52:1-9.
- Hogan SA, Chaurin V, O'Kennedy BT, Kelly PM. 2012. Influence of dairy proteins on textural changes in high-protein bars. *Int Dairy J* 26:58-65.
- Huppertz T, Hogan S. 2015. Milk protein ingredients for controlling hardening of protein bars. *J Dairy Sci* 98(Suppl. 2):541.
- Imtiaz SR, Kuhn-Sherlock B, Campbell M. 2012. Effect of dairy protein blends on texture of high protein bars. *J Texture Stud* 43(4):275-86.
- Kelly GM, O'Mahony JA, Kelly AL, Huppertz T, Kennedy D, O'Callaghan DJ. 2015. Influence of protein concentration on surface composition and physico-chemical properties of spray-dried milk protein concentrate powders. *Int Dairy J* 51:34-40.
- Li R, Roos YH, Miao S. 2016. Roles of particle size on physical and mechanical properties of dairy model solids. *J Food Eng* 173:69-75.

- Li Y, Szlachetka K, Chen P, Lin X, Ruan R. 2008. Ingredient characterization and hardening of high-protein food bars: An NMR state diagram approach. *Cereal Chem* 85(6):780-6.
- Liu X, Zhou P, Tran A, Labuza TP. 2009. Effects of polyols on the stability of whey proteins in intermediate-moisture food model systems. *J Agric Food Chem* 57(6):2339-45.
- Loveday SM, Hindmarsh JP, Creamer LK, Singh H. 2010. Physicochemical changes in intermediate-moisture protein bars made with whey protein or calcium caseinate. *Food Res Int* 43(5):1321-8.
- Loveday SM, Hindmarsh JP, Creamer LK, Singh H. 2009. Physicochemical changes in a model protein bar during storage. *Food Res Int* 42(7):798-806.
- McMahon DJ, Adams SL, McManus WR. 2009. Hardening of high-protein nutrition bars and sugar/polyol-protein phase separation. *J Food Sci* 74(6):E312-21.
- Muttakin S, Kim MS, Lee D-U. 2015. Tailoring physicochemical and sensorial properties of defatted soybean flour using jet-milling technology. *Food Chem* 187:106-11.
- O'Mahony JA, Fox PF. 2013. Milk proteins: Introduction and historical aspects. In: McSweeney PLH, Fox PF, editors. *Advanced Dairy Chemistry: Volume 1A: Proteins: Basic Aspects*. 4th edition. p 43-85.
- Protonotariou S, Mandala I, Rosell CM. 2015. Jet milling effect on functionality, quality and in vitro digestibility of whole wheat flour and bread. *Food Bioprocess Tech* 8(6):1319-29.
- Protonotariou S, Drakos A, Evageliou V, Ritzoulis C, Mandala I. 2014. Sieving fractionation and jet mill micronization affect the functional properties of wheat flour. *J Food Eng* 134:24-9.
- Quinn JR, Paton D. 1979. A practical measurement of water hydration capacity of protein materials. *Cereal Chem* 56(1):38-40.

- Rao Q, Kamdar AK, Guo M, Labuza TP. 2016a. Effect of bovine casein and its hydrolysates on hardening in protein dough model systems during storage. *Food Control* 60:621-8.
- Rao Q, Kamdar AK, Labuza TP. 2016b. Storage stability of food protein hydrolysates - A review. *Crit Rev Food Sci*. 56 (7):1169-92.
- Roudaut G, Simatos D, Champion D, Contreras-Lopez E, Le Meste M. 2004. Molecular mobility around the glass transition temperature: a mini review. *Innov Food Sci Emerg* 5(2):127-34.
- Saleem IY, Smyth HDC. 2010. Micronization of a soft material: Air-jet and micro-ball milling. *AAPS PharmSciTech* 11(4):1642-9.
- Schuck P, Jeantet R, Dolivet A. 2012. Determination of rehydration ability. *Analytical Methods for Food and Dairy Powders*. United Kingdom: John Wiley & Sons, Ltd. p 203-15.
- Schuck P, Mejean S, Dolivet A, Gaiani C, Banon S, Scher J, Jeantet R. 2007. Water transfer during rehydration of micellar casein powders. *Le Lait* 87(4-5):425-32.
- Schwarzwälder S, Nied R, Sickel H. 2014. Dry fine grinding with jet mills: Potentials of energy optimization. *Chem Eng Technol* 37(5):806-12.
- Sun C, Liu R, Wu T, Liang B, Shi C, Zhang M. 2015a. Effect of superfine grinding on the structural and physicochemical properties of whey protein and applications for microparticulated proteins. *Food Sci Biotechnol* 24(5):1637-43.
- Sun C, Wu T, Liu R, Liang B, Tian Z, Zhang E, Zhang M. 2015b. Effects of superfine grinding and microparticulation on the surface hydrophobicity of whey protein concentrate and its relation to emulsions stability. *Food Hydrocolloid* 51:512-8.
- Walstra PW, Jan TM, Geurts TJ. 2005. *Milk Properties*. Dairy Science and Technology. 2nd Edition. Boca Raton: CRC Press Taylor and Francis Group. p 159-174.

Zhou P, Liu D, Chen X, Chen Y, Labuza TP. 2014. Stability of whey protein hydrolysate powders: Effects of relative humidity and temperature. *Food Chem* 150:457-62.

Zhou P, Liu X, Labuza TP. 2008a. Effects of moisture-induced whey protein aggregation on protein conformation, the state of water molecules, and the microstructure and texture of high-protein-containing matrix. *J Agric Food Chem* 56(12):4534-40.

Zhou P, Liu X, Labuza TP. 2008b. Moisture-induced aggregation of whey proteins in a protein/buffer model system. *J Agric Food Chem* 56(6):2048-54.

1 **Tables**

2 **Table 1. Particle size diameters¹, span values², densities³, and air volumes⁴ for control, jet-milled (JM), and freeze-dried (FD)**

3 **MPC85**

MPC85 ⁵	D ₁₀	D ₅₀	D ₉₀	D _{4,3}	S	ρ_{loose}	ρ_{100X}	ρ_{1250X}	ρ_{particle}	V _{oa}	V _{ia}
Control	18 ^a	67 ^a	179 ^a	86 ^a	2.4 ^a	0.32 ^b	0.37 ^b	0.41 ^c	1.08 ^c	20.5 ^a	182 ^a
JM-Fine	1 ^c	7 ^d	16 ^d	8 ^d	2.0 ^d	0.38 ^a	0.39 ^b	0.48 ^b	1.33 ^a	3.3 ^c	181 ^a
JM-Coarse	2 ^c	19 ^c	44 ^c	22 ^c	2.3 ^b	0.33 ^b	0.37 ^b	0.47 ^b	1.31 ^b	4.7 ^b	192 ^a
FD	11 ^b	39 ^b	97 ^b	49 ^b	2.2 ^c	0.41 ^a	0.50 ^a	0.56 ^a	1.33 ^a	3.3 ^c	127 ^b

4 ¹ D₁₀, D₅₀, and D₉₀ are the diameters (μm) where 10%, 50%, and 90% of all powder particles have smaller size, respectively. D_{4,3} is the volume-weighted mean
 5 diameter (μm) for the distribution.

6 ² S represents particle size distribution span, a unit less value used to describe distribution width.

7 ³ ρ_{loose} , ρ_{100X} , ρ_{1250X} , and ρ_{particle} are loose, tapped, extremely tapped, and particle densities (g/cm³), respectively.

8 ⁴ V_{oa} and V_{ia} are occluded and interstitial air volumes (mL/100 g), respectively.

9 ⁵ Control, spray dried milk protein concentrate with 85% protein (MPC85). JM-Fine, finely jet-milled MPC85. JM-Coarse, coarsely jet-milled MPC85. FD,
 10 freeze-dried MPC85.

11 ^{a-d} Least squares means are significantly different ($P < 0.05$) if they do not share a common superscript within the same column.

12 **Table 2. Water holding capacity (WHC)¹ and dispersibility index (DI)² of control, jet-**
13 **milled (JM), and freeze-dried (FD) MPC85**

MPC85 ³	WHC	DI
Control	3.4 ^a	44.8 ^b
JM-Fine	3.2 ^{ab}	65.6 ^a
JM-Coarse	3.0 ^b	72.4 ^a
FD	3.1 ^b	68.8 ^a

14 ¹ WHC, water held per solid mass (g/g).

15 ² DI, percent solids that pass a 212-micron mesh after dispersion in Millipore water (%).

16 ³ Control, spray dried milk protein concentrate with 85% protein (MPC85). JM-Fine, finely jet-milled MPC85. JM-
17 Coarse, coarsely jet-milled MPC85. FD, freeze-dried MPC85.

18 ^{a,b} Least squares means are significantly different ($P < 0.05$) if they do not share a common superscript within the
19 same column.

20 **Table 3. Water droplet contact angle¹ and volume² on surfaces made from control, jet-**
 21 **milled (JM), and freeze-dried (FD) MPC85 during dynamic contact analysis**

MPC85 ³	θ_{0s}	θ_{420s}	$d\theta/dt$	V_{0s}	V_{420s}	dV/dt
Control	69 ^{ab,z}	41 ^{b,y}	-2.23 ^a	2.9 ^{b,z}	2.0 ^{b,y}	-0.12 ^{ab}
JM-Fine	76 ^{a,z}	58 ^{a,y}	-2.39 ^a	4.2 ^{a,z}	3.2 ^{a,y}	-0.14 ^a
JM-Coarse	67 ^{b,z}	52 ^{a,y}	-1.89 ^a	3.6 ^{ab,z}	2.7 ^{ab,y}	-0.13 ^{ab}
FD	67 ^{b,z}	53 ^{a,y}	-1.49 ^a	4.1 ^{a,z}	3.3 ^{a,y}	-0.11 ^b

22 ¹ θ_{0s} , initial contact angle (°). θ_{420s} , contact angle after 420 s (°). $d\theta/dt$, contact angle change with respect to time
 23 (°/min).

24 ² V_{0s} , initial water droplet volume (μL). V_{420s} , water droplet volume after 420 s (μL). dV/dt , water droplet volume
 25 change with respect to time (μL/min).

26 ³ Control, spray dried milk protein concentrate with 85% protein (MPC85). JM-Fine, finely jet-milled MPC85. JM-
 27 Coarse, coarsely jet-milled MPC85. FD, freeze-dried MPC85.

28 ^{a,b} Least squares means are significantly different ($P < 0.05$) if they do not share a common superscript within the
 29 same column.

30 ^{y,z} Least squares means are significantly different ($P < 0.05$) if they do not share a common superscript within the
 31 same row for each variable.

32 **Table 4. High-protein nutrition bar hardness¹ after storage at 22°C or 32°C for the indicated number of days**

MPC85 ²	Day 0	22°C					32°C				
		Day 6	Day 13	Day 20	Day 29	Day 42	Day 6	Day 13	Day 20	Day 29	Day 42
Control	15 ^{c,z}	18 ^{c,z}	19 ^{c,z}	17 ^{c,z}	17 ^{c,z}	15 ^{c,z}	18 ^{c,z}	18 ^{c,z}	21 ^{b,z}	20 ^{c,z}	18 ^{c,z}
JM-Fine	56 ^{a,w}	56 ^{a,w}	58 ^{a,wx}	61 ^{a,wxxy}	67 ^{a,y}	65 ^{a,xy}	56 ^{a,w}	56 ^{a,w}	62 ^{a,wxxy}	62 ^{a,wxxy}	77 ^{a,z}
FD	33 ^{b,z}	34 ^{b,z}	33 ^{b,z}	33 ^{b,z}	33 ^{b,z}	34 ^{b,z}	28 ^{b,z}	28 ^{b,z}	29 ^{b,z}	32 ^{b,z}	31 ^{b,z}

33 ¹ Hardness (N) was the compressive force at 60% strain during the first compression.

34 ² High-protein nutrition bars were formulated at 30% protein (w/w) using a single milk protein concentrate with 85% protein (MPC85). Control, spray dried
 35 MPC85. JM-Fine, finely jet-milled MPC85. FD, freeze-dried MPC85.

36 ^{a-c} Least squares means are significantly different ($P < 0.05$) if they do not share a common superscript within the same column.

37 ^{w-z} Least squares means are significantly different ($P < 0.05$) if they do not share a common superscript within the same row.

38 **Table 5. High-protein nutrition bar fracturability¹ after storage at 22°C or 32°C for the indicated number of days**

MPC85 ²	Day 0	22°C					32°C				
		Day 6	Day 13	Day 20	Day 29	Day 42	Day 6	Day 13	Day 20	Day 29	Day 42
Control	15 ^{a,u}	19 ^{a,uv}	23 ^{a,uvw}	22 ^{a,uv}	24 ^{a,uvw}	27 ^{a,vw}	26 ^{a,vw}	31 ^{a,wx}	39 ^{a,xy}	46 ^{a,y}	56 ^{a,z}
JM-Fine	23 ^{a,w}	25 ^{a,wx}	27 ^{a,wx}	28 ^{a,wx}	30 ^{a,wxy}	32 ^{a,xy}	28 ^{a,wx}	32 ^{a,wxy}	33 ^{a,xy}	38 ^{a,y}	49 ^{a,z}
FD	19 ^{a,v}	23 ^{a,vw}	24 ^{a,vwx}	24 ^{a,vwx}	26 ^{a,vwx}	26 ^{a,vwx}	25 ^{a,vwx}	28 ^{a,wxy}	33 ^{a,xy}	36 ^{a,yz}	43 ^{a,z}

39 ¹ Fracturability (N) was the compressive force when the sample yielded or cracked during the first compression.

40 ² High-protein nutrition bars were formulated at 30% protein (w/w) using a single milk protein concentrate with 85% protein (MPC85). Control, spray dried
 41 MPC85. JM-Fine, finely jet-milled MPC85. FD, freeze-dried MPC85.

42 ^{a-c} Least squares means are significantly different ($P < 0.05$) if they do not share a common superscript within the same column.

43 ^{u-z} Least squares means are significantly different ($P < 0.05$) if they do not share a common superscript within the same row.

44 **Table 6. High-protein nutrition bar maximum compressive force¹ after storage at 22°C or 32°C for the indicated number of**
 45 **days**

MPC85 ²	Day 0	22°C					32°C				
		Day 6	Day 13	Day 20	Day 29	Day 42	Day 6	Day 13	Day 20	Day 29	Day 42
Control	16 ^{c,v}	20 ^{b,vw}	23 ^{b,vw}	22 ^{b,vw}	24 ^{b,vw}	27 ^{b,vw}	26 ^{b,vw}	31 ^{b,wx}	39 ^{b,xy}	46 ^{b,yz}	56 ^{b,z}
JM-Fine	56 ^{a,y}	56 ^{a,y}	58 ^{a,y}	61 ^{a,y}	67 ^{a,yz}	65 ^{a,y}	56 ^{a,y}	56 ^{a,y}	62 ^{a,y}	62 ^{a,y}	77 ^{a,z}
FD	33 ^{b,yz}	34 ^{b,yz}	34 ^{b,yz}	33 ^{b,yz}	34 ^{b,yz}	34 ^{b,yz}	30 ^{b,y}	32 ^{b,y}	35 ^{b,yz}	41 ^{b,yz}	44 ^{b,z}

46 ¹ Maximum compressive force (N) was the larger of hardness or fracturability for each measurement.

47 ² High-protein nutrition bars were formulated at 30% protein (w/w) using a single milk protein concentrate with 85% protein (MPC85). Control, spray dried
 48 MPC85. JM-Fine, finely jet-milled MPC85. FD, freeze-dried MPC85.

49 ^{a-c} Least squares means are significantly different ($P < 0.05$) if they do not share a common superscript within the same column.

50 ^{v-z} Least squares means are significantly different ($P < 0.05$) if they do not share a common superscript within the same row.

51 **Table 7. High-protein nutrition bar adhesiveness¹ after storage at 22°C or 32°C for the indicated number of days**

MPC85 ²	Day 0	22°C					32°C				
		Day 6	Day 13	Day 20	Day 29	Day 42	Day 6	Day 13	Day 20	Day 29	Day 42
Control	0.04 ^{c,z}	0.03 ^{c,z}	0.02 ^{c,z}	0.01 ^{c,z}	0.02 ^{c,z}	0.01 ^{c,z}	0.02 ^{c,z}	0.02 ^{c,z}	0.01 ^{b,z}	0.01 ^{b,z}	0.00 ^{b,z}
JM-Fine	1.19 ^{a,z}	1.01 ^{a,yz}	1.07 ^{a,z}	0.68 ^{a,vwx}	0.85 ^{a,xy}	0.80 ^{a,wxy}	0.74 ^{a,vwx}	0.54 ^{a,v}	0.54 ^{a,v}	0.70 ^{a,vwx}	0.63 ^{a,vw}
FD	0.44 ^{b,z}	0.41 ^{b,yz}	0.40 ^{b,yz}	0.40 ^{b,yz}	0.40 ^{b,yz}	0.38 ^{b,xyz}	0.27 ^{b,xyz}	0.26 ^{b,xyz}	0.24 ^{b,xyz}	0.22 ^{b,xy}	0.18 ^{b,x}

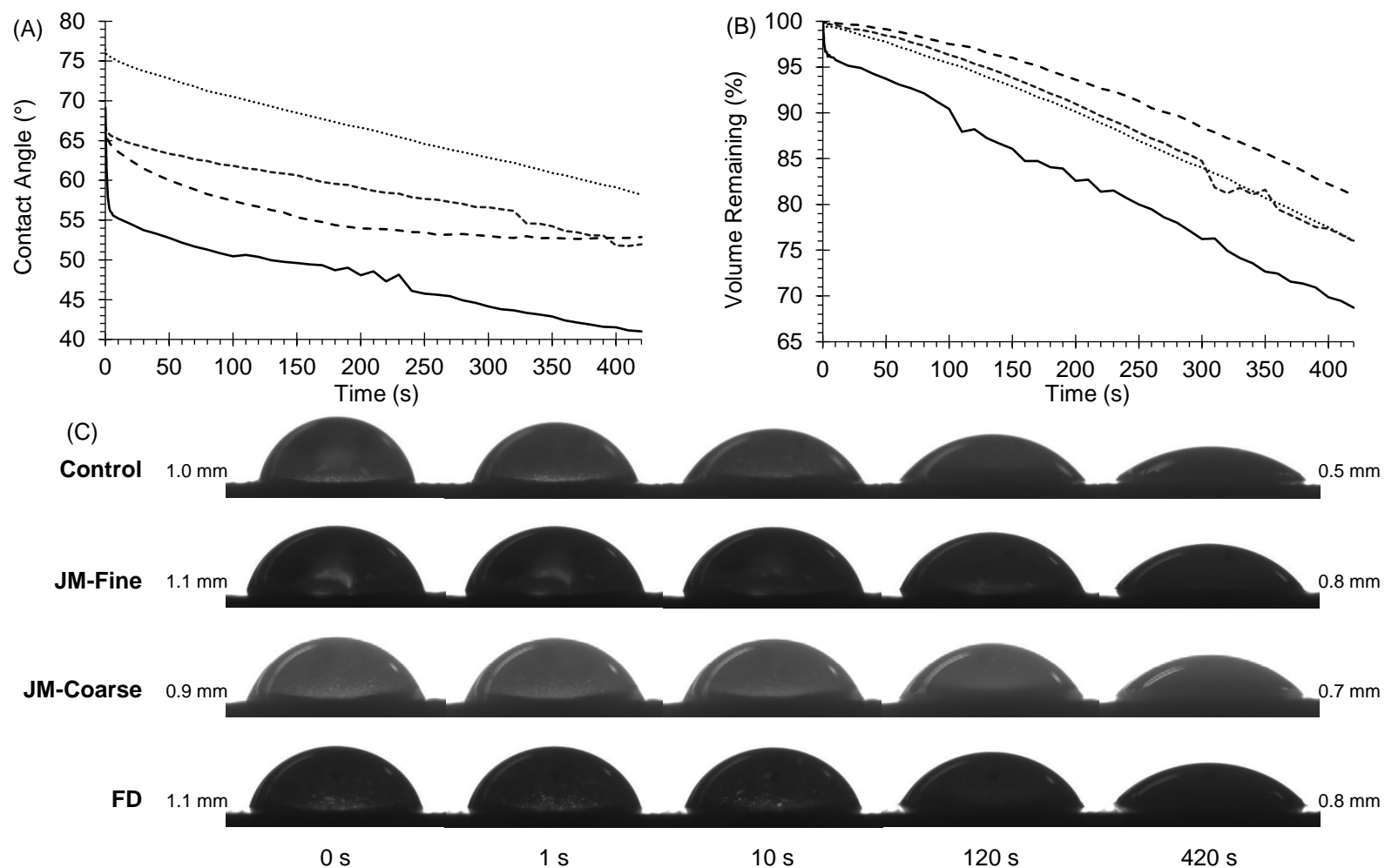
52 ¹ Adhesiveness (J) was the absolute area under the curve during crosshead withdrawal after the first compression.

53 ² High-protein nutrition bars were formulated at 30% protein (w/w) using a single milk protein concentrate with 85% protein (MPC85). Control, spray dried
 54 MPC85. JM-Fine, finely jet-milled MPC85. FD, freeze-dried MPC85.

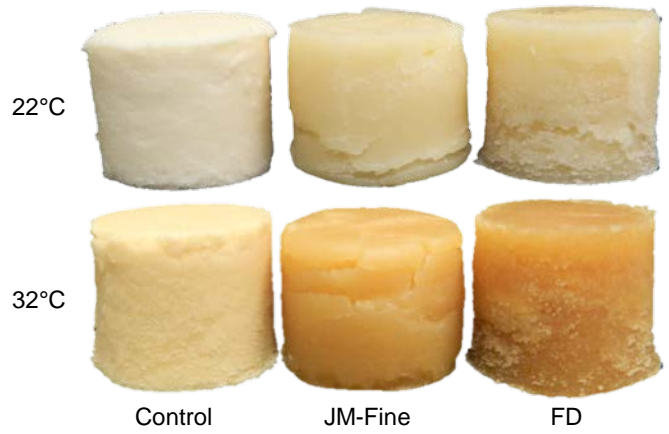
55 ^{a-c} Least squares means are significantly different ($P < 0.05$) if they do not share a common superscript within the same column.

56 ^{v-z} Least squares means are significantly different ($P < 0.05$) if they do not share a common superscript within the same row.

57 **Figures**

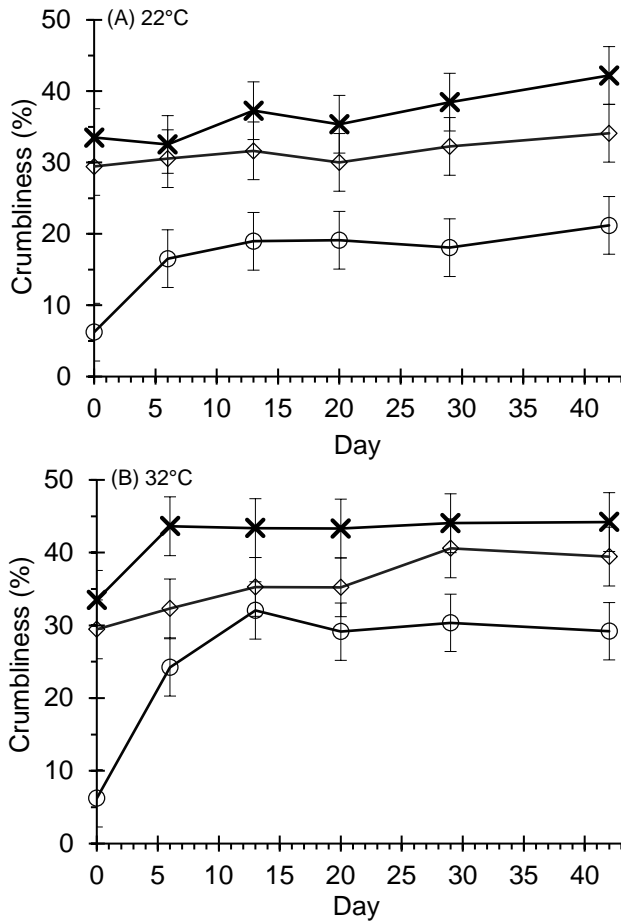


58 **Figure 1–Contact angle (A), volume remaining (B), and representative side view (C) of a water droplet on a pressed surface**
 59 **made from control, jet-milled (JM), and freeze-dried (FD) MPC85 during dynamic contact angle analysis.** Control (—), spray
 60 dried milk protein concentrate with 85% protein (MPC85). JM-Fine (···), finely jet-milled MPC85. JM-Coarse (---), coarsely jet-
 61 milled MPC85. FD (— · —), freeze-dried MPC85. Droplet height (mm) at 0 s and after 420 s is specified in image C.

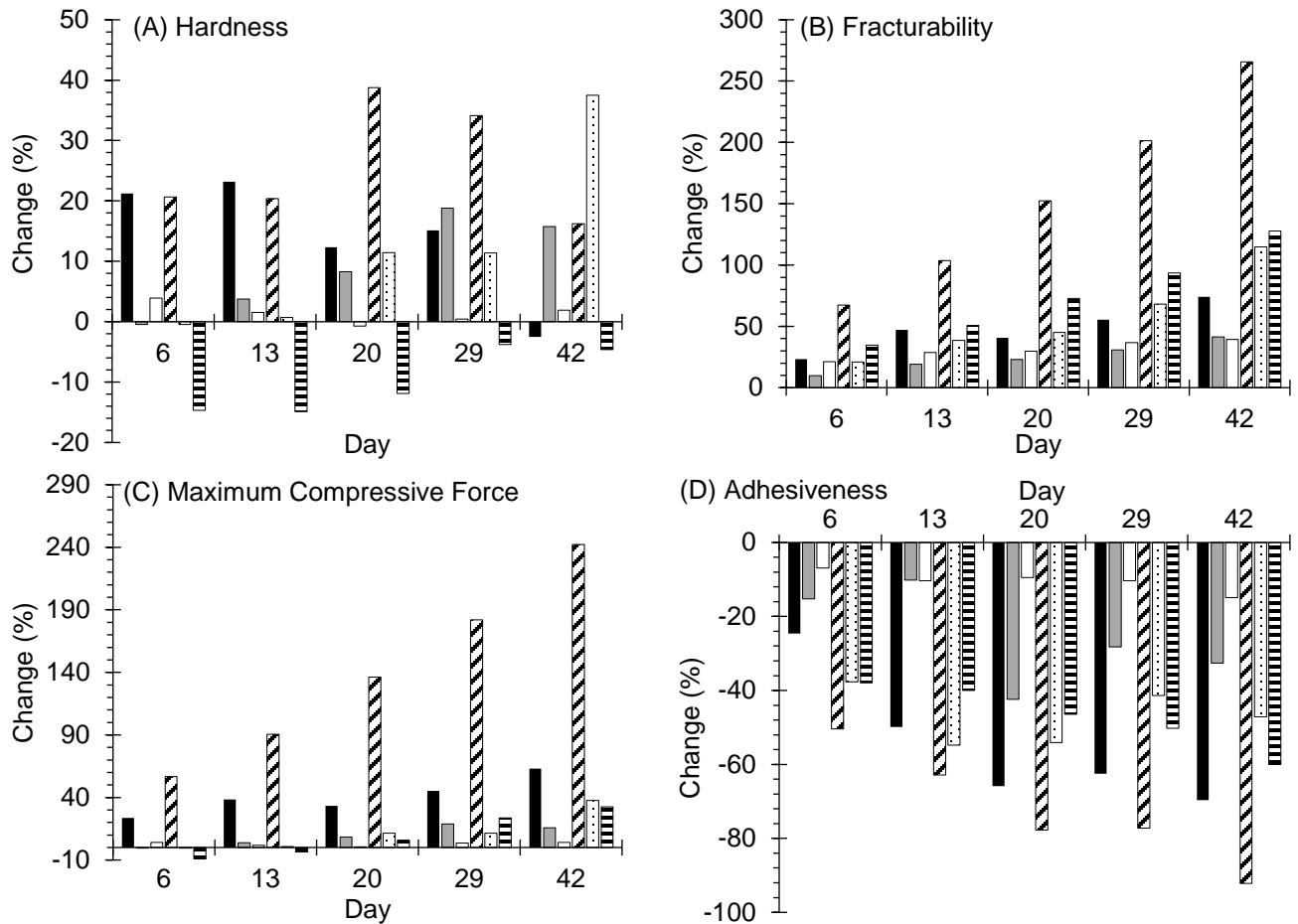


62

63 **Figure 2—The high-protein nutrition bars after 42 days at 22°C or 32°C.** High-protein
64 nutrition bars were formulated at 30% protein (w/w) using a single milk protein concentrate with
65 85% protein (MPC85). Control, spray dried MPC85. JM-Fine, finely jet-milled MPC85. FD,
66 freeze-dried MPC85.



67 **Figure 3—High-protein nutrition bar crumbliness after storage at 22°C (A) or 32°C (B) for**
 68 **the indicated number of days.** Crumbliness was the average mass percent (%) passing a 5.6
 69 mm aperture. High-protein nutrition bars were formulated at 30% protein (w/w) using a single
 70 milk protein concentrate with 85% protein (MPC85). Control (×), spray dried MPC85. JM-Fine
 71 (○), finely jet-milled MPC85. FD (◇), freeze-dried MPC85. Error bars represent ± SE.



72 **Figure 4—Average percent change in high-protein nutrition bar hardness (A), fracturability (B),**
 73 **maximum compressive force (C), and adhesiveness (D) after storage at 22°C or 32°C for the**
 74 **indicated number of days with respect to day 0.** High protein nutrition bars were formulated at 30%
 75 protein (w/w) using a single milk protein concentrate with 85% protein (MPC85). Control, spray dried
 76 MPC85. JM-Fine, finely jet-milled MPC85. FD, freeze-dried MPC85.
 77 22°C storage: ■ Control, ■ JM-Fine, □ FD. 32°C storage: ▨ Control, ▩ JM-Fine, ▪ FD.